[10] I. S. Gradshteyn and I. W. Ryzhik, *Table of Integrals, Series and Products*. New York: Academic Press, 1965, pp. 38–40.
[11] J. J. H. Wang, "An analytical approach for use with waveguide enzyme-inactivation investigations," Final report, U. S. army Medical R & D Command Grant DAMD17-77-G-7422, Engineering Experiment Station, Georgia Institute of Technology, Jan. 1978.
[12] M. J. Hagmann, O. P. Gandhi, and C. H. Durney, "Upper bound on cell size for moment-method solutions," *IEEE Trans. Microwave Theory Tech.*, vol. MTT-25, pp. 831–832, Oct. 1977.

Method of Analysis and Filtering Properties of Microwave Planar Networks

GUGLIELMO D'INZEO, FRANCO GIANNINI, CESARE M. SODI, AND ROBERTO SORRENTINO, MEMBER, IEEE

Abstract—**A method of analysis of planar microwave structures, based on a field expansion in term of resonant modes, is presented. A first advantage of the method consists in the possibility of taking into account fringe effects by introducing, for each resonant mode, an equivalent model of the structure. Moreover, the electromagnetic interpretation of the filtering properties of two-port networks, particularly of the transmission zeros, whose nature has been the subject of several discussions, is easily obtained. The existence of two types of transmission zeros, modal and interaction zeros is pointed out. The first ones are due to the structure's resonances, while the second ones are due to the interaction between resonant modes. Several experiments performed on circular and rectangular microstrips in the frequency range 2–18 GHz have shown a good agreement with the theory.**

I. Introduction

AFTER THE STUDY of the transmission properties of microstrip lines, the great diffusion of microwave integrated circuits has led to the analysis of general planar circuits. To this purpose, analytical methods, applied to structures of simple geometry [1]–[3], and numerical methods, apt to the study of more complex geometries [4]–[6], have been developed. In both cases a magnetic wall model has been adopted for the structure because of the formidable boundary value problems. In such a way, however, one not only neglects the dispersion properties of the circuit, which are due to fringe effects, but often obtains erroneous results [7].

To overcome this difficulty, in the case of step discontinuities, i.e., of structures with separable geometry in rectangular coordinates, Menzel and Wolff [8] have recently proposed a method of analysis based on the correction of the magnetic wall model by means of frequency dependent effective parameters. However, it must be observed that effective parameters depend not only on the frequency, but also on the field distribution inside the structure. It is sufficient to instance the disk resonators for which Wolff and Knoppik [9] have shown a frequency dependent equivalent model to exist for each resonant mode, in such a way that a unique equivalent model for the structure cannot be defined. This fact strongly limits the applicability of all the analyses of microstrip structures presented until now. Considerable attention has been devoted to nonuniform lines, i.e., lines with continuously or not continuously varying cross sections. The existence of transmission zeros has been stressed both theoretically and experimentally. In the particular case of a double step discontinuity, the physical nature of such zeros has been discussed for a long time [2], [10]–[13] and they have been ascribed to the excitation of higher order modes of propagation in the line section between the two discontinuities. As will be shown below, such an interpretation, in our opinion, is not correct, also because transmission zeros are present in generic nonuniform lines where the EM field cannot propagate as exp $(-j\beta z)$.

In this paper an analysis of planar circuits based on the theory of resonant cavities is presented. Three important advantages are so obtained. The first consists in the possibility of introducing frequency dependent effective parameters for each resonant mode of the structure in such a way as to obtain an accurate characterization of its frequency behavior. The second is an electromagnetic interpretation of the network's filtering properties, particularly of the transmission zeros, is easily obtained and the above mentioned problems are clarified. Finally, the present method leads to the evaluation of the impedance matrix of the network in the form of a partial fraction expansion with the advantages pointed out by Silvester [6].

The analysis is limited to the important case of two-port networks, since the extension to the general case is

Manuscript received May 16, 1977; revised December 7, 1977. This work has been supported in part by the Consiglio Nazionale delle Ricerche (C. N. R.), Italy.

The authors are with the Istituto di Elettronica, Università di Roma, Rome, Italy.

0018-9480/78/0700-0462$00.75

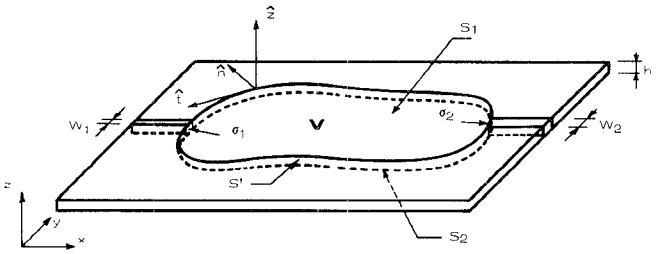

Fig. 1. The planar two-port circuit.

straightforward. The general filtering properties are discussed and criteria for locating transmission zeros are given. Several experimental results for circular and rectangular structures in the frequency range 2–18 GHz show a good agreement with the theoretical ones, obtained using the effective parameters proposed in [9]. Structures with nonseparable geometries could also be studied with the same technique through a numerical method (e.g., a finite element method).

II. Formulation of Field Problem

Fig. 1 shows a microstrip two-port circuit. The main difficulty in the study of such a structure is due to the fact that it is an open one, i.e., the EM field extends to infinity. The central section may be considered as an open resonator; the EM field is mainly concentrated in the cylindrical volume V bounded by the two conducting surfaces S_1 and S_2 and, laterally, by the cylindrical surface S'. It may be expressed as a function of the tangential magnetic field $\boldsymbol{H}_\tau$ on S' in terms of the modes of the cavity V. Following a procedure analogous to that of Kurokawa [14], one obtains

$$\boldsymbol{E}=\Sigma_a e_a \boldsymbol{E}_a+\Sigma_\alpha e_\alpha \boldsymbol{E}_\alpha \tag{1}$$

$$\boldsymbol{H}=\Sigma_a h_a \boldsymbol{H}_a+\Sigma_\alpha h_\alpha \boldsymbol{H}_\alpha \tag{2}$$

where $\boldsymbol{E}_a$ and $\boldsymbol{E}_\alpha$ are the orthonormalized eigenvectors of the following eigenvalue problem:

$$\nabla\times\nabla\times\boldsymbol{E}-\nabla\nabla\cdot\boldsymbol{E}-k^2\boldsymbol{E}=0, \quad \text{inside } V \tag{3a}$$

$$\boldsymbol{n}\times\boldsymbol{E}=0 \qquad \nabla\cdot\boldsymbol{E}=0, \quad \text{on } S_1, S_2 \tag{3b}$$

$$\boldsymbol{n}\cdot\boldsymbol{E}=0 \qquad \boldsymbol{n}\times\nabla\times\boldsymbol{E}=0, \quad \text{on } S' \tag{3c}$$

with the further conditions:

$$\nabla\cdot\boldsymbol{E}_a=0 \qquad \nabla\times\boldsymbol{E}_a\neq 0, \quad \text{inside } V \tag{4a}$$

$$\nabla\times\boldsymbol{E}_\alpha=0, \quad \text{inside } V. \tag{4b}$$

Similarly, $\boldsymbol{H}_a$ and $\boldsymbol{H}_\alpha$ are the orthonormalized eigenvectors of

$$\nabla\times\nabla\times\boldsymbol{H}-\nabla\nabla\cdot\boldsymbol{H}-k^2\boldsymbol{H}=0, \quad \text{inside } V \tag{5a}$$

$$\boldsymbol{n}\cdot\boldsymbol{H}=0 \qquad \boldsymbol{n}\times\nabla\times\boldsymbol{H}=0, \quad \text{on } S_1, S_2 \tag{5b}$$

$$\boldsymbol{n}\times\boldsymbol{H}=0 \qquad \nabla\cdot\boldsymbol{H}=0, \quad \text{on } S' \tag{5c}$$

with the conditions

$$\nabla\cdot\boldsymbol{H}_a=0 \qquad \nabla\times\boldsymbol{H}_a\neq 0, \quad \text{inside } V \tag{6a}$$

$$\nabla\times\boldsymbol{H}_\alpha=0, \quad \text{inside } V. \tag{6b}$$

It is possible to demonstrate that the eigenvalues of (3)–(4) coincide with those of (5)–(6) and that

$$\nabla\times\boldsymbol{H}_a=k_a\boldsymbol{E}_a$$

$$\nabla\times\boldsymbol{E}_a=k_a\boldsymbol{H}_a. \tag{7}$$

The coefficient of the expansions (1) and (2) may be calculated imposing that the EM field satisfies Maxwell's equations. One obtains

$$e_a=\frac{j\omega\mu}{k_a^2-\omega^2\mu\epsilon}\int_{S'}\boldsymbol{n}\times\boldsymbol{H}_\tau\cdot\boldsymbol{E}_a\,dS$$

$$h_a=\frac{-k_a}{j\omega\mu}e_a$$

$$e_\alpha=\frac{1}{j\omega\mu}\int_{S'}\boldsymbol{n}\times\boldsymbol{H}_\tau\cdot\boldsymbol{E}_\alpha\,dS$$

$$h_\alpha=0. \tag{8}$$

Once the set of eigenvalue of (3) and (5) is known, the evaluation of the EM field inside V depends on the knowledge of the tangential magnetic field $\boldsymbol{H}_\tau$ on S'. In a first approximation we may assume that $\boldsymbol{H}_\tau$ is different from zero only at the connections σ_i between the cavity and the lines where it has a TEM distribution[1]. Thus it is constant. However, $\boldsymbol{H}_\tau$ is not exactly zero on the remainder of S'; fringe effects can be taken into account by ascribing to the structure effective dimensions and an effective permittivity, according to the widely adopted magnetic wall model of microstrip structures. We shall come back to this point later.

Because of the above simplifying hypotheses, the EM field in the cavity is determined as a function of the magnetic field $\boldsymbol{H}_{\tau 1}=H_1\boldsymbol{t}$ and $\boldsymbol{H}_{\tau 2}=H_2\boldsymbol{t}$ at the outputs, which is independent of z. The structure may, therefore, be considered as a two-dimensional one. It is easily seen that, imposing the condition $\partial/\partial_z=0$ on (1)–(8), the $\boldsymbol{E}_a$'s have only the z component, while the $\boldsymbol{E}_\alpha$'s do not exist, with the exception of only the mode $\boldsymbol{E}_0$ having zero divergence. After simple manipulations, the EM field in the cavity may be expressed as follows:

$$\boldsymbol{E}=\hat{z}\Sigma_a e_a E_a+\hat{z}\,e_0 V^{-1/2} \tag{9}$$

$$\boldsymbol{H}=\frac{1}{j\omega\mu}\Sigma_a e_a\hat{z}\times\nabla_t E_a \tag{10}$$

where

$$e_a=\frac{j\omega\mu}{k_a^2-\omega^2\mu\epsilon}\left(\sqrt{\sigma_1}\,P_{a_1}H_1+\sqrt{\sigma_2}\,P_{a_2}H_2\right) \tag{11a}$$

$$P_{ai}=\sigma_i^{-1/2}\int_{\sigma_i}E_a\,dS, \qquad i=1,2 \tag{11b}$$

$$e_0=\frac{V^{-1/2}}{j\omega\epsilon}(\sigma_1 H_1+\sigma_2 H_2) \tag{11c}$$

where $\hat{z}$ is the unit vector of the z axis, V is the volume of

[1]Higher order modes on the uniform lines may be neglected with good approximation if the uniform sections are long enough and their widths are much smaller than the cavity's dimension [1]. In any case, when necessary, higher modes can be taken into account with a rather more complicate algebra.

the cavity, and σ_1 and σ_2 are the surfaces of the outputs of the cavity, i.e., the portions of S' where $\boldsymbol{H}_\tau$ is different from zero. $\boldsymbol{E}_0 = \hat{z}V^{-1/2}$ is the mode having zero curl and zero divergence, belonging to the $\boldsymbol{E}_\alpha$'s. Since (11c) can be obtained from (11a) and (11b) by putting $k_a^2 = 0$ and $E_a = E_0 = V^{-1/2}$, later on this mode will be included among the E_a's.

The eigenfunctions E_a have to satisfy the two-dimensional eigenvalue equation deriving from (3)

$$\nabla_t^2 E + k^2 E = 0 \tag{12}$$

together with the boundary condition

$$\frac{\partial E}{\partial n} = 0 \tag{12'}$$

which derives from the second of (3c); the other boundary conditions are automatically satisfied.

One can note that the a modes are, in this case, TM with respect to the z direction; the o mode, on the contrary, corresponds to the electrostatic field problem.

Once (12) is solved for a particular geometry, the EM field inside the cavity is fully determined through (9)–(11) as a function of the magnetic fields supported by the uniform lines. Nevertheless, a terminal description of the structure as a two-port network is generally preferable. This can be obtained by evaluating the impedance matrix, relative, of course, to the dominant TEM modes of the lines. The amplitude of the electric field E_i on the ith line is obtained by projecting the field (9), calculated at σ_i, on the abstract vector space of the modes of the line and retaining the TEM component [15], i.e.,

$$E_i = \frac{1}{\sigma_i}\int_{\sigma_i} \hat{z}\cdot\boldsymbol{E}\, dS, \qquad i = 1,2.$$

Through (9) and (11) E_i can be expressed as a function of H_1, H_2

$$\begin{aligned} E_1 &= H_1 j\omega\mu\Sigma_a \frac{P_{a1}^2}{k_a^2 - \omega^2\mu\epsilon} \\ &\quad + H_2 j\omega\mu\Sigma_a \frac{P_{a1}P_{a2}}{k_a^2 - \omega^2\mu\epsilon}\cdot\left[\sigma_2/\sigma_1\right]^{1/2} \\ E_2 &= H_1 j\omega\mu\Sigma_a \frac{P_{a2}P_{a1}}{k_a^2 - \omega^2\mu\epsilon}\cdot\left[\sigma_1/\sigma_2\right]^{1/2} \\ &\quad + H_2 j\omega\mu\Sigma_a \frac{P_{a2}^2}{k_a^2 - \omega^2\mu\epsilon}. \end{aligned} \tag{13}$$

If one defines equivalent voltages and currents in such a way as to normalize to unity the characteristic impedances of the lines, i.e.,

$$\begin{aligned} V_i &= E_i\left[\sigma_i\sqrt{\epsilon/\mu}\,\right]^{1/2} \\ I_i &= H_i\left[\sigma_i\sqrt{\mu/\epsilon}\,\right]^{1/2}, \qquad i = 1,2 \end{aligned} \tag{14}$$

from (13) and (14) the following expression of the $[Z]$ matrix is easily obtained

$$[Z] = \Sigma_a [Z_a] \tag{15}$$

with

$$[Z_a] = \frac{j\omega c}{\omega_a^2 - \omega^2}\begin{bmatrix} P_{a1}^2 & P_{a1}P_{a2} \\ P_{a2}P_{a1} & P_{a2}^2 \end{bmatrix} \tag{15'}$$

μ and ϵ are the substrate's permeability and permittivity, respectively, and

$$\omega_a = ck_a$$

are the resonant frequencies of the cavity. If there are ν_a linearly independent eigenfunctions corresponding to the same eigenvalue k_a^2

$$E_a^{(1)}, E_a^{(2)}, \cdots E_a^{(\nu_a)}$$

which, without loss of generality, may be supposed to be ortogonal, (15') should be replaced by

$$[Z_a] = \frac{j\omega c}{\omega_a^2 - \omega^2}\sum_{\nu=1}^{\nu_a}\begin{bmatrix} P_{a1}^{(\nu)^2} & P_{a1}^{(\nu)}P_{a2}^{(\nu)} \\ P_{a1}^{(\nu)}P_{a2}^{(\nu)} & P_{a2}^{(\nu)^2} \end{bmatrix}, \qquad c = 1/\sqrt{\mu\epsilon} \tag{15''}$$

while, in (15), the summation over a should include only distinct ω_a's. $[Z]$ is a purely imaginary matrix since the structure has been supposed without losses. If the network is symmetrical

$$P_{a2} = \epsilon_a P_{a1} \tag{16}$$

where $\epsilon_a = 1$ for even modes and $\epsilon_a = -1$ for odd modes. The impedance parameters may be written

$$\begin{aligned} Z_{11} &= Z_{22} = Z_{ev} + Z_{od} \\ Z_{12} &= Z_{21} = Z_{ev} - Z_{od} \end{aligned} \tag{17}$$

where

$$\begin{aligned} Z_{ev} &= j\omega c\Sigma \frac{P_{ev}^2}{\omega_{ev}^2 - \omega^2} \\ Z_{od} &= j\omega c\Sigma \frac{P_{od}^2}{\omega_{od}^2 - \omega^2} \end{aligned} \tag{17'}$$

ev being the index of the even modes, od of the odd modes.

The calculation of the $[Z]$ matrix requires the evaluation of the eigenfunctions and eigenvalues E_a, k_a^2 and then of the P_{a1}. This can be done analytically if the structure has a separable geometry; if the geometry is not separable, a numerical method could be adopted.

III. General Filtering Properties

The formulation given in the previous section has led to a complete characterization of the microwave network in terms of its impedance matrix. In order to discuss the filtering properties of the structure, a description in terms of the scattering parameters is preferable since the impedance matrix elements are not quantities easily measurable at microwave frequencies; moreover the scattering matrix provides a more appropriate physical description of the structure behavior. In terms of the impedance parameters the scattering parameters are given by

$$s_{11}=\left[(Z_{11}-1)(Z_{22}+1)-Z_{12}^2\right]/D$$
$$s_{22}=\left[(Z_{11}+1)(Z_{22}-1)-Z_{12}^2\right]/D$$
$$s_{12}=s_{21}=2Z_{12}/D \tag{18}$$

where

$$D=(Z_{11}+1)(Z_{22}+1)-Z_{12}^2. \tag{18'}$$

Let us start examining the structure's behavior at the resonant frequency ω_p of one of the modes. It is convenient to write the Z parameters as follows:

$$Z_{11}=j\omega c\frac{Q_{11}}{\omega_p^2-\omega^2}+\hat{Z}_{11}$$
$$Z_{22}=j\omega c\frac{Q_{22}}{\omega_p^2-\omega^2}+\hat{Z}_{22}$$
$$Z_{12}=j\omega c\frac{Q_{12}}{\omega_p^2-\omega^2}+\hat{Z}_{12} \tag{19}$$

where $\hat{Z}_{ij}$ remains finite for $\omega\to\omega_p$. Let us distinguish two cases.

1) $Q_{11}Q_{22}=Q_{12}^2$. This equality is always verified for nondegenerate modes. We further distinguish two subcases.

a) $Q_{11}Q_{22}=Q_{12}^2=0$. Since the case $Q_{11}=Q_{22}=Q_{12}=0$ may be excluded ,[2] the structure has to be nonsymmetrical ($Q_{11}\neq Q_{22}$). From (18) and (19) one immediately obtains

$$s_{12}(\omega_p)=0.$$

According to whether Q_{11} or Q_{22} is different from zero, $s_{11}=1$, or $s_{22}=1$, respectively. The resonant frequency ω_p, therefore, corresponds to a transmission zero. This can be easily explained from an electromagnetic point of view. Suppose $Q_{22}=0$: this means that the p mode is uncoupled to the second port. When an EM field is incident to the first port at the frequency $\omega=\omega_p$, the EM field inside the cavity would become infinite (see (11a)) unless the total (incident plus reflected) magnetic field at the first port is zero; this implies $s_{11}=1$, $s_{12}=0$.

We may, therefore, conclude that in nonsymmetrical structures a transmission zero takes place at the resonant frequency of one mode which is uncoupled to one of the ports. Later on, transmission zeros taking place at resonant frequencies ω_a will be referred to as modal zeros.

b) $Q_{11}Q_{22}=Q_{12}^2\neq 0$. In this case, when $\omega\to\omega_p$ the scattering parameters do not generally assume significant values. Nevertheless, it is worth considering the case of a symmetrical structure ($Q_{11}=Q_{22}=\pm Q_{12}$). For $\omega\to\omega_p$ one obtains from (18) and (19)

$$s_{11}=s_{22}=\frac{\hat{Z}_{11}-\epsilon_p\hat{Z}_{12}}{1+\hat{Z}_{11}-\epsilon_p\hat{Z}_{12}} \qquad s_{12}=s_{21}=\frac{\epsilon_p}{1+\hat{Z}_{11}-\epsilon_p\hat{Z}_{12}}.$$

According to whether p is an even ($\epsilon_p=1$) or an odd ($\epsilon_p=-1$) mode the quantity $\hat{Z}_{11}-\epsilon_p\hat{Z}_{12}$ is equal to $2Z_{od}$ or to $2Z_{ev}$ (see (17')), respectively. These quantities are often negligible with respect to unity, so that $s_{11}=s_{22}\cong 0$, $s_{12}\cong\epsilon_p$. In other words, in a symmetrical nondegenerate structure modal transmission zeros do not take place; on the contrary, the ω_a's give generally place to approximate reflection zeros. It is worth specifying that the existence of a reflection zero at or near ω_p depends on the widths of the ports; in some cases, in fact, the reflection zero takes place only if the ports are small enough. Typical examples will be shown below. For the sake of brevity we omit to demonstrate the above statements which, on the other hand, can be easily proved.

2) $Q_{11}Q_{22}\neq Q_{12}^2$. This case can be verified only for a degenerate mode. It is easily seen that at the frequency $\omega=\omega_p$ $s_{11}=s_{22}=1$, $s_{12}=0$. This is another case of modal transmission zero, which is due to a degenerate mode of the cavity, or rather to the superposition of degenerate modes.

Having examined the structure's behavior at the resonant frequencies of the cavity, let us now consider the cases when a transmission zero takes place.

From (18) it follows that for s_{12} to be zero there are only two cases: a) $|D|=\infty$. This condition holds only if $\omega=\omega_a$, and therefore is that of a modal transmission zero. b) $Z_{12}=0$. Since

$$Z_{12}=j\omega c\Sigma_a\frac{P_{a1}P_{a2}}{\omega_a^2-\omega^2} \tag{20}$$

it can be easily inferred that between two consecutive resonant frequencies ω_p, ω_q such that [3]

$$\operatorname{sgn}(P_{p1}P_{p2})=\operatorname{sgn}(P_{q1}P_{q2}) \tag{21}$$

there is necessarily a frequency $\omega_z\in(\omega_p,\omega_q)$ such that

$$Z_{12}(\omega_z)=0,\quad s_{12}(\omega_z)=0.$$

In case of mode degeneracy, (21) should be replaced by

$$\operatorname{sgn}\left(\sum_{\nu=1}^{\nu_p}I_{p1}^{(\nu)}I_{p2}^{(\nu)}\right)=\operatorname{sgn}\left(\sum_{\nu=1}^{\nu_q}I_{q1}^{(\nu)}I_{q2}^{(\nu)}\right). \tag{21'}$$

In order to find a physical interpretation of this type of transmission zero, suppose the cavity is excited by a field incident to the first port at a frequency located between ω_p and ω_q; if (21) is satisfied, the p and q modes will give place to opposite contributions to the field at the output. In other words, they interact destructively at the second port. At the frequency $\omega=\omega_z$, whose location between ω_p and ω_q depends also on the contribution of all the other modes, there is a totally destructive interaction in such a way that no power can be transferred towards the output. This type of transmission zero will be called interaction zero.

For symmetrical nondegenerate structures, because of (16), (21) becomes

[2] In that case, in fact, the p mode cannot be excited in the structure and therefore can be excluded from any consideration.

[3] If $P_{q1}P_{q2}=0$ (i.e., there is a modal transmission zero at ω_q), in (21) the successive mode must be considered, say, the r mode, such that $P_{r1}P_{r2}\neq 0$.

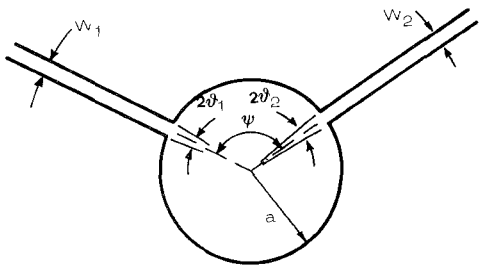

Fig. 2. The circular microstrip.

$$\epsilon_p = \epsilon_q$$

i.e., if two consecutive resonant modes are both even or odd, an interaction transmission zero is located between their resonant frequencies.

IV. The Circular Microstrip

The first case of the two-port network we have considered is the circularly shaped microstrip line shown in Fig. 2. The orthonormalized eigenfunctions of (12) are, in this case,

$$E_{mn} = C_{mn} J_m(k_{mn} r) \begin{Bmatrix} \cos m\phi \\ \sin m\phi \end{Bmatrix}, \qquad \begin{matrix} m = 0,1,2\cdots \\ n = 1,2,3\cdots \end{matrix} \tag{22}$$

where

$$C_{mn} = \frac{1}{\sqrt{V}\, J_m(\xi'_{mn})} \left[\frac{\delta_m}{1 - \left(\frac{m}{\xi'_{mn}}\right)^2} \right]^{1/2}$$

$$V = \pi a^2 h$$

$$k_{mn} = \xi'_{mn}/a = \omega_{mn}/c$$

and

$$\delta_m = \begin{cases} 1, & \text{for } m = 0 \\ 2, & \text{for } m \neq 0 \end{cases}$$

is the Neumann factor; ξ'_{mn} is the nth root of the equation

$$\frac{d}{dx} J_m(x) = 0$$

and h is the substrate's thickness. Besides the set of eigenfunctions (22), the eigenfunction corresponding to $k^2 = 0$ must be considered

$$E_{00} = 1/\sqrt{V}\,.$$

Such an eigenfunction can be obtained from (22) by putting conventionally

$$\left.\frac{m}{\xi'_{mn}}\right|_{\substack{n=0 \\ m=0}} = 0.$$

Equation (22) shows the existence of a pair of degenerate modes for any $m \neq 0$. We shall restrict our attention to the important case of symmetrical structures ($w_1 = w_2 = w$; $\theta_1 = \theta_2 = \theta$). Following the procedure described in the previous section, one obtains for the $[Z]$ matrix elements[4]

$$Z_{11} = Z_{22} = j\omega c \frac{4\theta^2}{\pi w} \sum_{m=0}^{\infty} \sum_{n=0}^{\infty} \frac{A_{mn}^2}{\omega_{mn}^2 - \omega^2}$$

$$Z_{21} = Z_{12} = j\omega c \frac{4\theta^2}{\pi w} \sum_{m=0}^{\infty} \sum_{n=0}^{\infty} \frac{A_{mn}^2}{\omega_{mn}^2 - \omega^2} \cos m\psi \tag{23}$$

where

$$A_{mn}^2 = \left(\frac{\sin m\theta}{m\theta}\right)^2 \frac{\delta_m}{1 - (m/\xi'_{mn})^2}. \tag{23'}$$

Let us consider the structure's behavior at the resonant frequencies of the cavity. The condition of case 2) of the previous section becomes

$$\cos^2 m\psi \neq 1. \tag{24}$$

Therefore, for generic values of ψ and for $m \neq 0$, each resonant frequency corresponds to a modal transmission zero. On the contrary, if $m\psi = s\pi$ ($s = 0,1,2,\cdots$) case 2b) is verified, i.e., for θ small enough, a reflection zero takes place near such resonant frequencies. This happens for all the modes of a doubly symmetrical structure ($\psi = \pi$) and, in general, for the $(0,n)$ modes.

Besides modal transmission zeros, interaction zeros take place between consecutive resonant frequencies $\omega_{m_1 n_1}$ and $\omega_{m_2 n_2}$ such that[5]

$$\operatorname{sgn}(\cos m_1\psi) = \operatorname{sgn}(\cos m_2\psi). \tag{25}$$

In the doubly symmetrical case ($\psi = \pi$) (31) becomes[6]

$$(-1)^{m_1} = (-1)^{m_2} \tag{25'}$$

i.e., an interaction zero is located between the resonant frequencies of two consecutive modes having both an even, or an odd, azimutal dependence.

From (25) it follows that transmission zeros can be located between any pair of resonant frequencies by varying the angle ψ between the two uniform lines.

Fig. 3 shows the theoretical behavior of the scattering parameter $|s_{12}|$ of a doubly symmetrical circular microstrip versus the frequency in the range 2–18 GHz. (Expressions (23) have been evaluated taking into account the first 62 modes). This curve has been obtained completely neglecting fringe effects, i.e., ascribing to the EM model the physical dimension of the structure and assuming for ϵ the permittivity of the substrate (alumina, $\epsilon = 10\ \epsilon_0$). The locations of the resonant frequencies ω_{mn} are also indicated in the figure. The structure presents two transmission zeros, which are due to the interaction between the pair of modes (2,1)–(0,1) and (1,2)–(5,1), accordingly to (25'). (The last resonant frequency is not indicated in the figure, because it is out of scale). Reflection zeros are located near each resonant frequency, with the exception of the modes (4,1) and (1,2) which are very close together; for the assumed port widths, corresponding to

[4]As a consequence of the hypothesis that the widths of the ports are much smaller than the cavity's radius, the arcs θ_1 and θ_2 may be confused with the corresponding chord.

[5]If $\cos m_2\psi = 0$, (thus a modal transmission zero takes place at $\omega_{m_2 n_2}$) the successive mode must be considered in (25). See footnote 3.

[6]It may be noted that in this case the structure behaves as a nondegenerate one, since for each k_{mn}^2 only one of the two degenerate modes can be excited, both from the input or from the output.

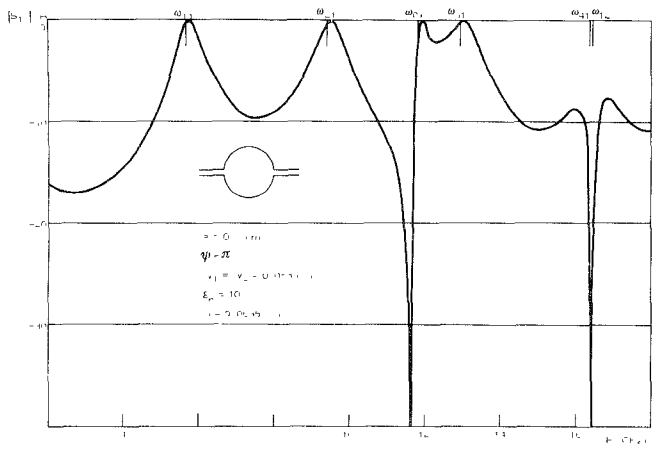

Fig. 3. Transmission coefficient $|s_{12}|$ versus the frequency for a circular microstrip (magnetic wall model without effective parameters).

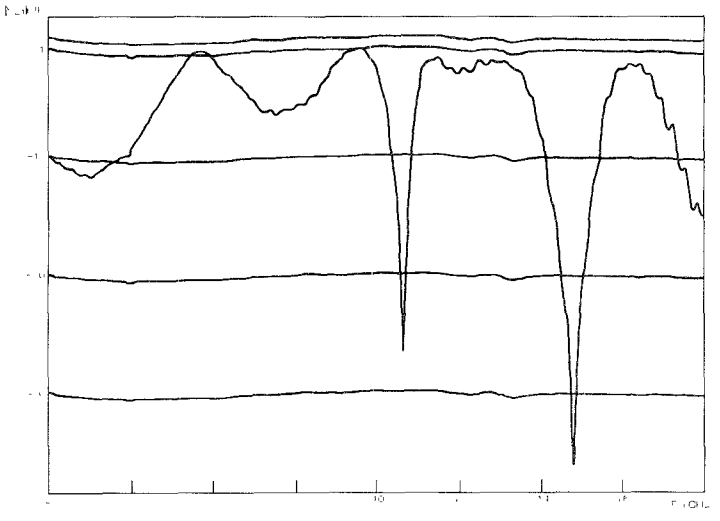

Fig. 4. Experimental behavior of the transmission coefficient $|s_{12}|$ versus the frequency for the same structure as in Fig. 3. Substrate material alumina.

50-Ω lines, reflection zeros do not take place at these frequencies.

Fig. 4 shows the experimental behavior of $|s_{12}|$ for the same structure as in Fig. 3. The comparison between these diagrams shows a good qualitative agreement between theory and experiment up to ~12 GHz. The disagreement consists on the one hand in a slight shifting of the reflection and transmission zero frequencies and, on the other hand, in lower values of the theoretical $|s_{12}|$. The latter fact can be easily explained, since the EM coupling between the uniform lines and the cavity is, in reality, stronger than the theory predicts, because the fringing field of the lines has been neglected. With regard to the frequency shifting of the two diagrams, it must be observed that the experimental resonant frequencies are different from the theoretical ones, as previously pointed out. Over ~12 GHz, the theory yields to inacceptable errors; the two diagrams do not agree even from a qualitative point of view. As has been previously noted [7], the experimental resonant frequencies may differ from the theoretical ones in such a way that the sequence of modes

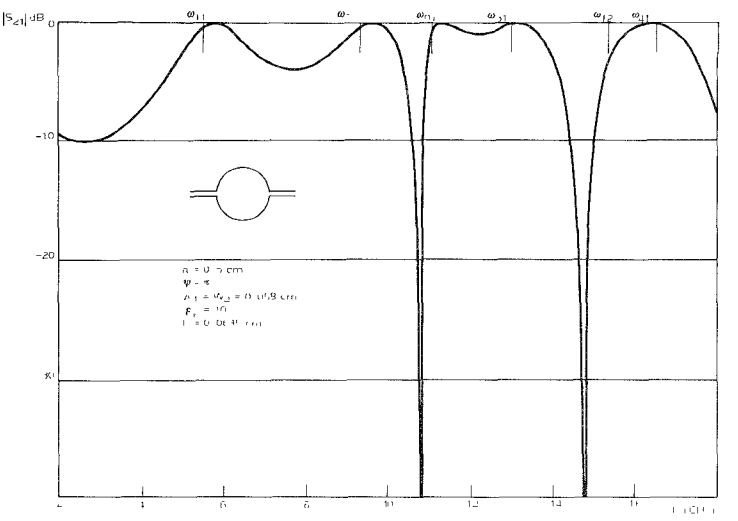

Fig. 5. Transmission coefficient $|s_{12}|$ versus the frequency for the same structure as in Fig. 3 (magnetic wall model according to the present theory).

is different in the two cases. Since interaction zeros depend on such a sequence, their location might be strongly altered.

The above considerations indicate that account must be taken of fringe effects both of the lines and of the cavity. This can be done by ascribing to the lines effective widths and effective permittivities accordingly, for instance, to Wheeler [16] or to Schneider [17], [18]. With regard to the circular resonator, fringe effects depend on the resonant mode and can be taken into account through an equivalent model for each mode, accordingly to Wolff and Knoppik [9]. Expressions (23) should be therefore modified by introducing an effective port width w_{eff}, an effective frequency dependent permittivity of the lines $\epsilon_{\text{eff}}(f)$, an effective cavity radius r_{eff} and, finally, an effective dynamic permittivity of the cavity $\epsilon_{\text{dyn},mn}(f)$, which also depends on the resonant mode.

The results obtained in this way are shown in Fig. 5 and agree very well with the experiments in Fig. 4. In particular, one can note that the resonant frequencies of the modes (4, 1) and (1, 2) are now interchanged: the second transmission zero is therefore due to the interaction between the (3, 1) and (1, 2) modes. This phenomenon is analogous to the modal inversion in circular waveguides [19] and could be experimentally verified by means of a field mapping technique [20]. The residual differences between the theoretical and experimental magnitudes of $|s_{12}|$ are essentially due to losses, particularly to radiation losses, which have been completely neglected.

Fig. 6(a) and (b) shows the theoretical behavior of $|s_{12}|$ versus the frequency for a circular microstrip with $\psi = \pi/2$. This structure presents a modal transmission zero at each resonant frequency of one mode having an odd azimutal dependence (see (24)), i.e., in the frequency range considered, of the modes (1, 1), (3, 1), and (1, 2). For $\psi = \pi/2$, (25) shows that interaction zeros take place between the resonant frequencies of modes $(4m_1, n_1) - (4m_2, n_2)$ or $(4m_1 + 2, n_1) - (4m_2 + 2, n_2)$; in the present case

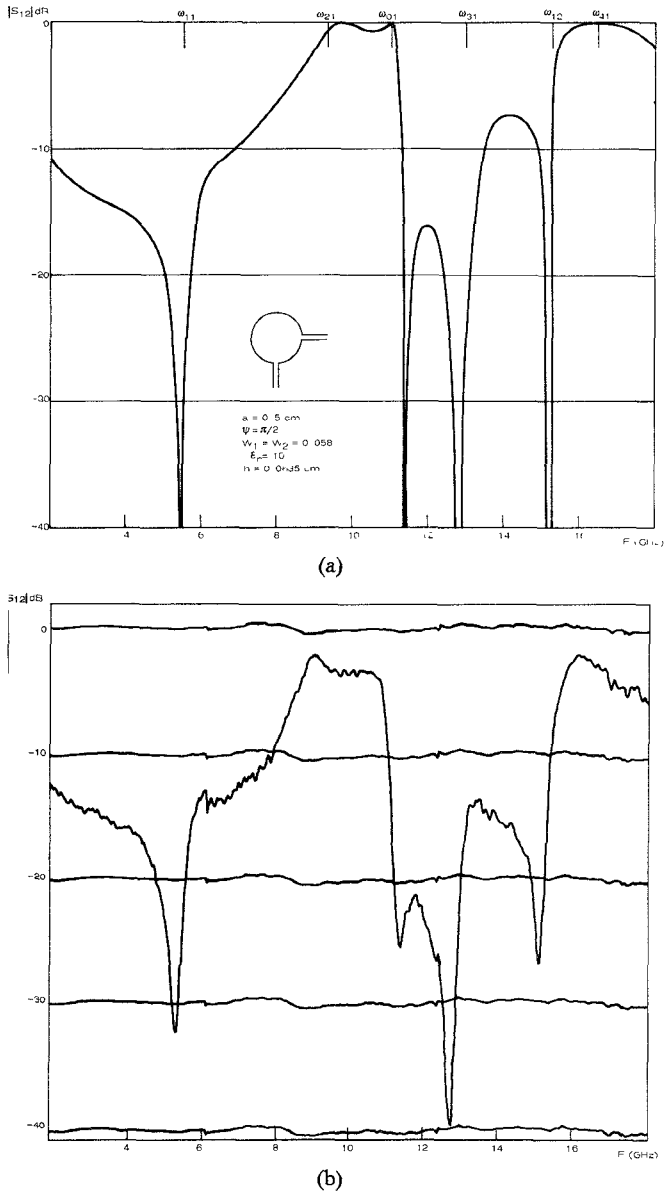

Fig. 6. Transmission coefficient $|s_{12}|$ versus the frequency, for a circular microstrip. (a) Theory. (b) Experiment.

there is only one interaction zero between the modes (0, 1) and (4, 1).

It is easy to verify that, for $\psi < \pi/2$, an interaction zero takes place between the (0, 0) and (1, 1) modes. For $\psi \to \pi/2$ the interaction zero tends to the modal zero due to the (1, 1) mode. Fig. 7 shows the theoretical frequency location of such transmission zero as a function of the angle ψ for a given cavity's radius. As can be seen, a good agreement with the experiments is obtained. This figure shows the possibility of locating a transmission zero at a given frequency by suitably positioning the output port of the network.

V. The Rectangular Microstrip

Another type of two-port planar network consists of a rectangular central section connected with two uniform lines (Fig. 8). This structure may be considered also as a

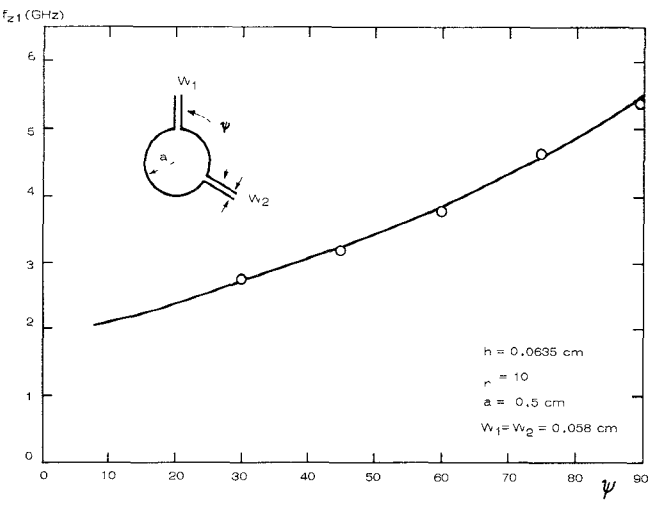

Fig. 7. Frequency location of the first transmission zero presented by a circular microstrip as a function of the angle between the two ports.

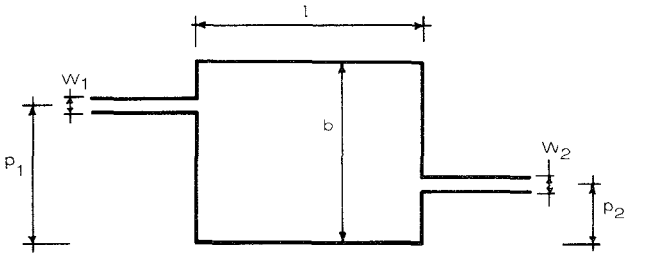

Fig. 8. The rectangular microstrip.

double step discontinuity; on the other hand, for $1 \ll b$ it becomes a stub structure.

Simple calculations yield to the following expressions of the Z parameters of the structure[7]

$$Z_{11} = \frac{j\omega c w_1}{b1} \sum_{m=0}^{\infty} \sum_{n=0}^{\infty} \frac{\delta_m \delta_n f_{n1}^2}{\omega_{mn}^2 - \omega^2}$$

$$Z_{22} = \frac{j\omega c w_2}{b1} \sum_{m=0}^{\infty} \sum_{n=0}^{\infty} \frac{\delta_m \delta_n f_{n2}^2}{\omega_{mn}^2 - w^2}$$

$$Z_{21} = Z_{12} = \frac{j\omega c \sqrt{w_1 w_2}}{b1} \sum_{m=0}^{\infty} \sum_{n=0}^{\infty} (-1)^m \frac{\delta_m \delta_n f_{n1} f_{n2}}{\omega_{mn}^2 - \omega^2} \quad (26)$$

where

$$\omega_{mn} = c\pi \sqrt{(m/1)^2 + (n/b)^2}$$

$$f_{ni} = \begin{cases} \cos \dfrac{n\pi p_i}{b} \dfrac{\sin \dfrac{n\pi w_i}{2b}}{\dfrac{n\pi w_i}{2b}}, & \text{for } n \neq 0 \\ 1, & \text{for } n = 0 \end{cases}.$$

[7]The series over m could be evaluated analytically and equivalent expressions to those in [1] would be obtained; nevertheless, they are not suitable for our purpose, since it is necessary to introduce effective parameters for each resonant mode, i.e., for each term of the series (26), in the same way as has been done in the case of the circular microstrip.

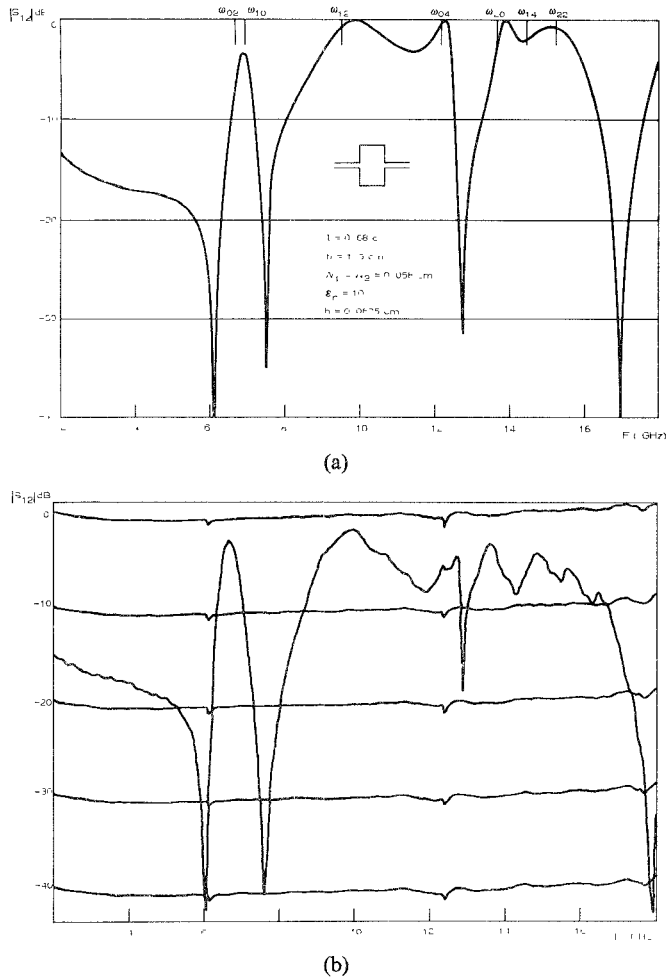

Fig. 9. Transmission coefficient $|s_{12}|$ versus the frequency for a symmetrical rectangular microstrip. (a) Theory. (b) Experiment.

For symmetrical structures ($w_1 = w_2$, $f_{n1}^2 = f_{n2}^2$), as previously stated, transmission zeros are only of the interaction type; in particular, if $p_1 = p_2$ condition (21) becomes

$$(-1)^{m_1} = (-1)^{m_2}$$

i.e., transmission zeros are located between the resonant frequencies of consecutive modes having both an even or an odd dependence with respect to the x direction.

Nonsymmetrical structures can also present modal transmission zeros, which are located at the resonant frequencies ω_{mn} such that $f_{n1} = 0$ and $f_{n2} \neq 0$, or vice versa.

Fig. 9(a) and (b) shows the theoretical and experimental behaviors of $|s_{12}|$ of a symmetrical rectangular microstrip versus the frequency in the range 2–18 GHz. Theoretical results have been obtained by adopting for the resonator the model suggested by Wolff and Knoppik [9]; the first 400 modes have been retained in (26). The structure presents four transmission zeros due to the interaction of the following pairs of modes: (0,0)–(0,2), (1,0)–(1,2), (0,4)–(2,0), (2,2)–(0,6). It is important to note that the first transmission zero is located close to the resonant frequency of the (0,2) mode. Since this frequency is nothing but the cutoff frequency of the $TE_{20}^{(x)}$ mode of propagation in the wider microstrip section, that transmission zero has been ascribed to the excitation of the $TE_{20}^{(x)}$ mode [10]–[12]. Such an interpretation is, in our opinion, inacceptable. As has been previously pointed out, given the symmetry of the structure, a resonant mode cannot give place to a transmission zero, but on the contrary it can give place to a reflection zero: the (0,2) mode can produce a transmission zero only through the interaction with another resonant mode, which is even with respect to the x direction (i.e., a $(2m,n)$ mode). For a different $1/b$ ratio, in fact, this mode does not give place to any transmission zero, as will be shown later. One may moreover observe that the (0,2) and (1,0) modes, which are rather close together, do not give place to any reflection zero. This is a typical case when two resonant modes interact together in such a way that no reflection zero takes place. However, one could verify that if the port widths would be very small (about 5μm) two reflection zeros would take place at these resonant frequencies.

The experimental results in Fig. 9(b) agree fairly well with the theoretical ones until ~12.5 GHz; at higher frequencies there is a little shifting between the theoretical and experimental resonant frequencies. Moreover, the effect of the losses becomes appreciable over ~15 GHz. A more accurate and complete model of the structure would therefore require a better evaluation of the resonant frequencies and, at the same time, the introduction of the losses.

In order to confirm what is stated above with regard to the (0,2) mode, another structure has been made with proper dimensions in such a way that this mode is located between two odd modes. Fig. 10(a) and (b) shows the corresponding theoretical and experimental results. As the theory predicts, in this case, the (0,2) mode does not give place to any transmission zero; the three transmission zeros are due to the interaction between the modes (4,0) and (2,2), (3,2) and (5,0), and (4,2) and (6,0). As can be noted the theory agrees very well with the experiment in the whole frequency range 2–18 GHz.

Fig. 11(a) and (b) shows the theoretical and experimental results for a nonsymmetrical rectangular microstrip. In this structure odd modes with respect to the y axis can be excited at the second port, but not at the first one. As a consequence, all the $(m,2n+1)$ modes give place to modal transmission zeros. It is worth observing that the first zero is located at the resonant frequency of the (0,1) mode, corresponding to the cutoff frequency of the $TE_{10}^{(x)}$ mode of propagation in the central section. This accounts for previous observations [10]–[13] with regard to nonsymmetrical step discontinuities; in this case, the statement that transmission zeros are due to higher order modes is correct, since it is a modal and not an interaction zero. The structure in Fig. 11 presents also three transmission zeros due to the interaction between the modes (2,0)–(0,2), (1,2)–(3,0), and (2,2)–(4,0). In spite of the complexity of the frequency behavior of the structure, the theoretical results may be considered highly satisfactory.

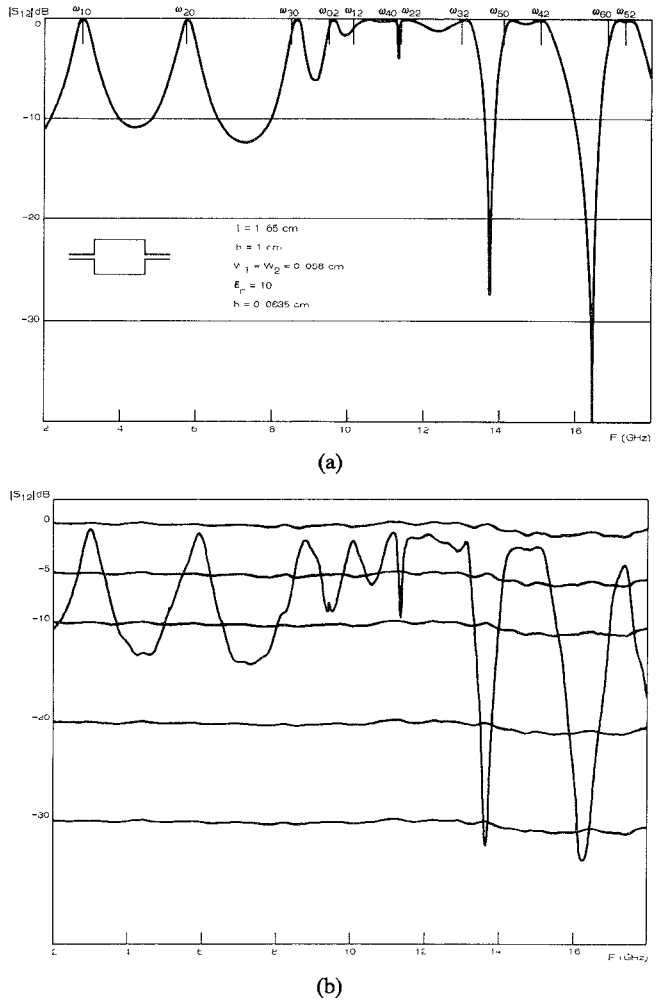

Fig. 10. Transmission coefficient $|s_{12}|$ versus the frequency for a symmetrical rectangular microstrip. (a) Theory. (b) Experiment.

VI. Conclusions

A method of analysis of planar microwave structures is presented, which is based on a field expansion in terms of resonant modes. The case of two-port networks is considered, but the extension to N-port circuits is straightforward. The general filtering properties are discussed and, in particular, the physical nature of transmission zeros, which has been the subject of several discussions, is clarified. The existence of two types of transmission zeros, modal and interaction zeros, is pointed out. The first ones are due to the structure's resonances, while the second ones are due to the interaction between resonant modes. The latter are the only ones present in symmetrical nondegenerate structures.

Fringe effects are accounted for in a simple way, namely by introducing in the magnetic wall model effective parameters for each resonant mode, while other methods presented until now are limited by the impossibility of taking into account fringe effects in an adequate way. It is also shown that these effects should not be neglected, since they can produce a modal inversion and, consequently, a strong alteration of the structure's frequency behavior.

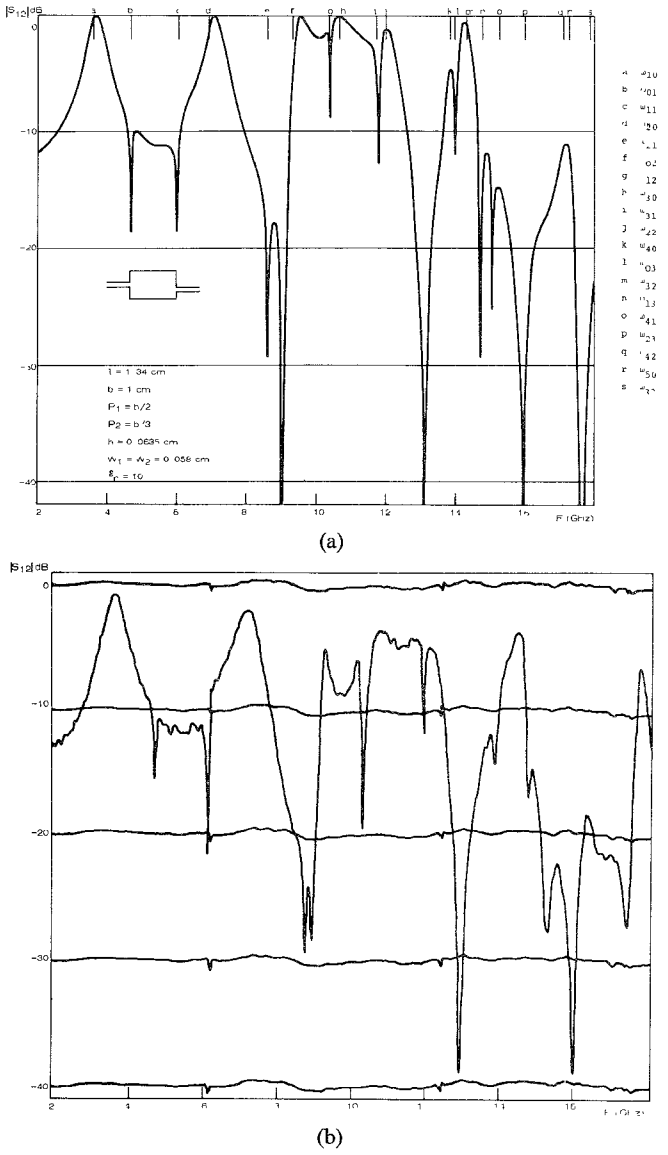

Fig. 11. Transmission coefficient $|s_{12}|$ versus the frequency for a nonsymmetrical rectangular microstrip. (a) Theory. (b) Experiment.

Several experimental results performed on circular and rectangular structures are compared with the theoretical ones deduced by assuming the effective parameters suggested in [9]. A good agreement is obtained, particularly for the circular microstrips; for rectangular microstrips a better characterization of the alterations due to fringing fields would be desirable. To that purpose it is necessary to adopt a full-wave analysis for calculating the resonant frequencies and the coupling between the lines and the resonant modes. This can be done on the basis of some methods presented in the literature [21]–[23].

Finally, it is worth pointing out that the method could be also adopted for planar circuits with any geometry, for instance through a finite element analysis.

Acknowledgment

The authors are indebted to the Servizio Microonde of the Elettronica S.p.a. for aid in the measurements; they also wish to thank B. De Santis for drawing the diagrams.

REFERENCES

[1] B. Bianco and S. Ridella, "Nonconventional transmission zeros in distributed rectangular structures," *IEEE Trans. Microwave Theory Tech.*, vol. MTT-20, pp. 297–303, May 1972.

[2] G. Kompa, "S-Matrix computation of microstrip discontinuities with a planar waveguide model," *Arch. Elek. Übertragung*, vol. 30, pp. 58–64, Feb. 1976.

[3] G. Kompa and R. Mehran, "Planar waveguide model for calculating microstrip components," *Electron. Lett.*, vol. 11, pp. 459–460, Sept. 1975.

[4] T. Okoshi, Y. Uehara, and T. Takeuchi, "The segmentation method—An approach to the analysis of microwave planar circuits," *IEEE Trans. Microwave Theory Tech.*, vol. MTT-24, pp. 662–668, Oct. 1976.

[5] T. Okoshi and T. Miyoshi, "The planar circuit—An approach to microwave integrated circuitry," *IEEE Trans. Microwave Theory Tech.*, vol. MTT-20, pp. 245–252, Apr. 1972.

[6] P. Silvester, "Finite-element analysis of planar microwave networks," *IEEE Trans. Microwave Theory Tech.*, vol. MTT-21, pp. 104–108, Feb. 1973.

[7] G. D'Inzeo, F. Giannini, and R. Sorrentino, "Theoretical and experimental analysis of non-uniform microstrip lines in the frequency range 2–18 GHz," in *Proc. of 6th European Microwave Con.* (Rome, Italy) pp. 627–631, 1976.

[8] W. Menzel and I. Wolff, "A method for calculating the frequency-dependent properties of microstrip discontinuities," *IEEE Trans. Microwave Theory Tech.*, vol. MTT-25, pp. 107–112, Feb. 1977.

[9] I. Wolff and N. Knoppik, "Rectangular and circular microstrip disk capacitors and resonators," *IEEE Trans. Microwave Theory Tech.*, vol. MTT-22, pp. 857–864, Oct. 1974.

[10] G. Kompa, "Excitation and propagation of higher modes in microstrip discontinuities," presented at *Proc. of 3th European Microwave Conf.*, Brussels, 1973.

[11] I. Wolff, G. Kompa, and R. Mehran, "Calculation methods for microstrip discontinuities and T-junctions," *Electron. Lett.*, vol. 8, pp. 177–179, Apr. 1972.

[12] B. Bianco, M. Granara, and S. Ridella, "Comments on the existence of transmission zeros in microstrip discontinuities," *Alta Frequenza*, vol. XLI, pp. 533E–534E, Nov. 1972.

[13] B. Bianco, M. Granara, and S. Ridella, "Filtering properties of two-dimensional lines' discontinuities," *Alta Frequenza*, vol. XLII, pp. 140E–148E, July 1973.

[14] K. Kurokawa, *An Introduction to the Theory of Microwave Circuits*. New York: Academic Press, 1969, ch. 4.

[15] P. M. Morse and H. Feshbach, *Methods of Theoretical-Physics*, vol. I. New York: McGraw-Hill, 1953, ch. 6, pp. 716–719.

[16] H. A. Wheeler, "Transmission-line properties of parallel wide strips separated by a dielectric sheet," *IEEE Trans. Microwave Theory Tech.*, vol. MTT-13, pp. 172–185, Mar. 1965.

[17] M. V. Schneider, "Microstrip lines for microwave integrated circuits," *Bell Syst. Tech. J.*, vol. 48, pp. 1421–1444, May 1969.

[18] ——, "Microstrip dispersion," *Proc. Inst. Elect. Electron. Engrs.*, vol. 60, pp. 144–146, 1972.

[19] G. N. Tsandoulas and W. J. Ince, "Modal inversion in circular waveguides—Part I: Theory and phenomenology," *IEEE Trans. Microwave Theory Tech.*, vol. MTT-19, pp. 386–392, Apr. 1971.

[20] F. Giannini, P. Maltese, and R. Sorrentino, "Liquid crystal technique for field detection in microwave integrated circuitry," *Alta Frequenza*, vol. XLVI, pp. 80E–88E, Apr. 1977.

[21] S. Akhtarzad and P. B. Johns, "Three-dimensional transmission-line matrix computer analysis of microstrip resonators," *IEEE Trans. Microwave Theory Tech.*, vol. MTT-23, pp. 990–997, Dec. 1975.

[22] R. Jansen, "High-order finite element polinomials in the computer analysis of arbitrarily shaped microstrip resonators," *Arch. Elek. Übertragung*, vol. 30, pp. 71–79, Feb. 1976.

[23] T. Itoh, "Analysis of microstrip resonators," *IEEE Trans. Microwave Theory Tech.*, vol. MTT-22, pp. 946–951, Nov. 1974.

Analysis of Planar Disk Networks

RENÉ R. BONETTI AND PLINIO TISSI

Abstract—**The impedance matrix of a disk n-port is determined with fringing fields at the disk edge included in the analysis. The theory is valid for both stripline and microstrip geometries and is also applicable to magnetic substrates. A simple quasi-static approximation to the disk capacitance is obtained. Applicability to numerical design is exemplified with the search for transmission zeros in a reciprocal 2 port. Experimental results are presented for the 1-port and 2-port disks.**

I. INTRODUCTION

PLANAR NETWORK theory is becoming a powerful tool for the design of microwave integrated circuits [1]–[4]. When compared to other physical structures, planar networks offer the designer considerable freedom, due not only to their size and shape but also to the large variety of devices realizable with simple geometries.

A very simple shape, the disk, has already proven very useful for the realization of junction circulators and presents interesting possibilities for other devices.

Well known theories for disk networks on magnetic substrate [5]–[7] make use of the edge magnetic wall (EMW) as a boundary condition at the disk edge and, therefore, exterior fields are not included in the analysis. With respect to this problem we quote Bosma [8]: "It is the unsolved problem of the fringing field that makes numerical design of circulators not yet very spectacular." Furthermore, in a recent paper by de Santis [9] transitions from volume modes to edge guided modes were shown to be strongly influenced by these fields.

Manuscript received March 1, 1977; revised September 22, 1977. This work was supported by contract FINEP-271-CT.

The authors are with the Instituto de Pesquisas Espaciais, Conselho Nacional de Desenvolvimento Cientifico e Tecnológico, São José dos Campos, SP, Brazil.

0018-9480/78/0700-0471$00.75